Acta Crystallographica Section F
Structural Biology Communications
ISSN 2053-230X

Preparation, purification, crystallization and preliminary crystallographic analysis of dual-domain β-propeller phytase from *Bacillus* sp. HJB17

Fang Lu,[a] Gangxin Guo,[a] Qianqian Li,[a] Duo Feng,[a] Yong Liu,[a] Huoqing Huang,[b] Peilong Yang,[b] Wei Gao[a,c]* and Bin Yao[b]*

[a]College of Science, Beijiing Forestry University, 35 Qinghuadong Road, Haidian District, Beijing 100083, People's Republic of China, [b]Key Laboratory for Feed Biotechnology of the Ministry of Agriculture, Feed Research Institute, Chinese Academy of Agricultural Sciences, Beijing, People's Republic of China, and [c]National Engineering Laboratory for Tree Breeding, Beijing Forestry University, 35 Qinghuadong Road, Haidian District, Beijing 100083, People's Republic of China

Correspondence e-mail: w_gao@bjfu.edu.cn, yaobin@mail.caas.net.cn

Received 9 August 2014
Accepted 5 November 2014

β-Propeller phytases (BPPs) are abundant in nature. Recently, dual-domain BPPs have been found in which the typical BPP domain is responsible for phytate hydrolysis. The dual-domain BPP (PhyH) from *Bacillus* sp. HJB17 was obtained with an incomplete N-terminal BPP domain (PhyH-DI; residues 41–318) and a typical BPP domain (PhyH-DII; residues 319–644) at the C-terminus. PhyH-DI was found to act synergistically (with a 1.2–2.5-fold increase in phosphate release) with PhyH-DII, other BPPs (PhyP and 168PhyA) and a histidine acid phosphatase. The structure of PhyH was therefore studied with the aim of explaining these functions. PhyH with the secreted signal peptide of the first 40 amino acids deleted (PhyHT) was cloned and expressed in *Escherichia coli*. Purified and active PhyHT protein was obtained by refolding from the precipitant. PhyHT was crystallized using the vapour-diffusion method. The crystal grew in a condition consisting of 0.2 *M* sodium acetate trihydrate, 0.1 *M* Tris–HCl pH 9.5, 25%(*w*/*v*) polyethylene glycol 4000 using 1 mg ml^{-1} protein solution at 289 K. A complete data set was collected from a crystal to 2.85 Å resolution using synchrotron radiation at 100 K. The crystal belonged to space group $P12_11$, with unit-cell parameters a = 46.82, b = 140.19, c = 81.94 Å, α = 90.00, β = 92.00, γ = 90.00°. The asymmetric unit was estimated to contain one molecule of PhyHT.

1. Introduction

Phytate, or *myo*-inositol hexakisphosphate (IP6), is one of the dominant organic phosphorus (P) compounds in nature and is very stable in soil. Phytate has anti-nutritional effects: in the intestines of animals, phytate can chelate a variety of metal ions such as Zn^{2+}, Ca^{2+}, Cu^{2+}, Fe^{2+}, Mg^{2+} and Co^{2+} and form insoluble complexes. Phytate can chelate nutrients such as proteins, amino acids and vitamins, decreasing their solubility, and thus affect the digestion and absorption of these nutrients by animals (Sharma *et al.*, 1978; Cowieson *et al.*, 2004). Owing to the high phosphate levels in manure and the accumulation of phosphorus at various locations, environmental pollution has raised serious concerns. Phytases appear to have significant value in effectively controlling phosphorus pollution. Phytase can degrade phytate gradually and generate lower inositol phosphate derivatives and inorganic phosphate (Mullaney *et al.*, 2000). Single-stomach animals and aquatic animals cannot effectively use the phosphorus from phytate because of a lack of phytase or low phytase enzyme activity (Pandey *et al.*, 2001). The β-propeller phytase family is the major class of phytases involved in the degradation of phytate (Cheng & Lim, 2006).

Low-phosphorus (P) stress is one of the major limiting factors in crop productivity. The application and promotion of phytase in research has important significance, as not only can it alleviate a shortage of phosphorus sources and reduce environmental pollution, but it also can promote the development of agriculture. These studies show that phytase may play an important role in the recycling of phosphorus.

Based on amino-acid sequence comparison, phytases can be classified into four classes: histidine acid phosphatase (HAP), purple acid

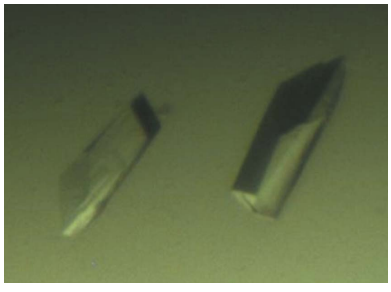

phosphatase (PAP), β-propeller phytase (BPP) and cysteine phosphatase (CP) (Lei *et al.*, 2007). A typical BPP has a six-bladed propeller fold with two phosphate-binding sites (a cleavage site and an affinity site) and six calcium-binding sites, three of which are high-affinity binding sites responsible for enzyme stability and the other three of which are low-affinity sites regulating the catalytic activity of the enzyme (Fu *et al.*, 2008; Kim *et al.*, 2010).

Among the four classes of phytases, BPP, with its neutral to alkaline pH optimum (pH 6.0–8.0), is a potential candidate for the hydrolysis of IP6 in aquatic environments with a near-neutral pH, such as seawater (pH of ~8.0) and lake water (pH slightly below 7.0). Recently, a new dual-domain BPP (PhyH) from *Bacillus* sp. HJB17 was identified to contain an incomplete N-terminal BPP domain (PhyH-DI; residues 41–318) and a typical BPP domain (PhyH-DII; residues 319–644) at the C-terminus (Li *et al.*, 2011).

Structures of phytase have been determined by many researchers. The structure of the thermostable phytase (TS-Phy) from *B. amyloliquefaciens* has been determined at 2.1 Å resolution in two different forms (Ha *et al.*, 2000). It has been shown that the binding of two calcium ions to high-affinity calcium-binding sites results in a dramatic increase in the thermostability and that the binding of three additional calcium ions to low-affinity calcium-binding sites at the top of the molecule initiates the catalytic activity of the enzyme.

A thermostable, calcium-dependent single-domain phytase from *Bacillus* has been identified that represents the first example of the β-propeller fold exhibiting phosphatase activity. Shin *et al.* (2001) successfully sought to delineate the catalytic mechanism and properties of this enzyme by determining its crystal structure. The enzyme reaction is likely to proceed through direct attack of the metal-bridging water molecule. The enzyme has two phosphate-binding sites: the 'cleavage site' and the 'affinity site'. They explain the puzzling formation of alternately dephosphorylated *myo*-inositol triphosphates from phytate and the hydrolysis of *myo*-inositol monophosphates.

Li *et al.* (2011) have shown that, compared with PhyH-DII, PhyH is catalytically more active against phytate (with a catalytic constant of 27.72 s^{-1} compared with 4.17 s^{-1}), which indicates the importance of PhyH-DI in phytate degradation. PhyH-DI was found to hydrolyze the phytate intermediate D-Ins(1,4,5,6)P4 and to act synergistically (with a 1.2–2.5-fold increase in phosphate release) with PhyH-DII, other BPPs (PhyP and 168PhyA) and a histidine acid phosphatase. Furthermore, fusion of PhyH-DI with PhyP or 168PhyA significantly enhanced their catalytic efficiencies. It may be that dual-domain BPPs have succeeded evolutionarily because they can increase the amount of available phosphate by interacting together. We therefore aimed to study the structure of PhyHT (PhyH with the secreted signal peptide of the first 40 amino acids deleted) in order to explain the mechanisms of these functions. In this paper, we report the expression, purification, crystallization and preliminary X-ray analysis of recombinant PhyHT.

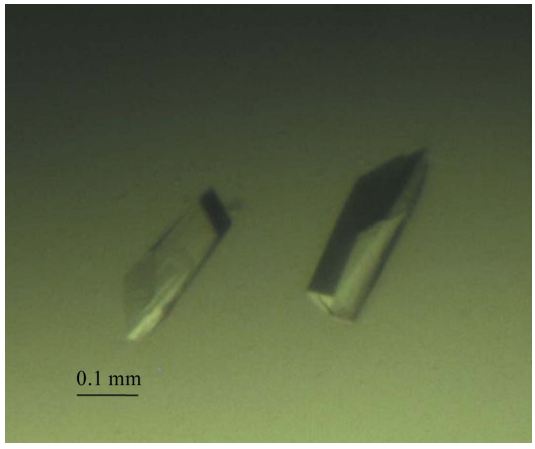

Figure 1
Crystal of PhyHT.

2. Materials and methods

2.1. Construction and expression of PhyHT

The expression vector pET-28b-PhyHT was produced as described by Li *et al.* (2011) with minor changes. Briefly, the gene for PhyHT (from *Bacillus* sp. HJB17) was amplified using PCR techniques with the PhyH gene (HM003049.1) as the template and was then ligated into the *Nde*I–*Xho*I sites of the pET-28b(+) vector, resulting in the recombinant vector pET-28b-PhyHT. The recombinant plasmid was transformed into *Escherichia coli* BL21 (DE3) competent cells. Positive transformants were grown in 5 ml LB medium pH 7.0 containing 100 µg ml^{-1} kanamycin overnight at 310 K. 20 ml aliquots of the overnight culture were subcultured into 1 l fresh LB medium containing kanamycin (100 µg ml^{-1}). Protein expression was induced by the addition of 0.2 m*M* isopropyl β-D-thiogalactopyranoside (IPTG) for 4–6 h at 310 K when the OD_{600} reached 0.6–0.8. The cell pellet was collected by centrifugation at 4000 rev min^{-1} for 30 min at 277 K, resuspended and ultrasonicated on ice for 10 min with phenylmethylsulfonyl fluoride (PMSF) added to the buffer to a final concentration of 1 m*M*. Gradient gel electrophoresis demonstrated that PhyHT was expressed in substantial quantities. No phytase activity was detected in the supernatant and pellet. PhyHT was found to have a apparent molecular weight of 69.3 kDa. The results show that recombinant PhyHT was only detected in the inclusion cell fraction (Fig. 2). We varied the construct, cells, culture temperature, IPTG concentration and culture time to attempt to obtain soluble protein; however, all attempts failed.

2.2. Refolding and purification of PhyHT

The inclusion cell fraction was refolded as described by Gao *et al.* (2014). Briefly, the bacterial pellet was ultrasonicated on ice for 10 min. After centrifugation at 13 000 rev min^{-1} and 277 K for 30 min, the inclusion body (inclusion cell fraction) was refolded by dialysis after washing and dissolution in the buffer described by Gao *et al.* (2014). A solution of refolded protein was obtained. The phytase activity of this solution was determined by measuring the amount of phosphate released from InsP6 using a modified ferrous sulfate molybdenum blue method (Holman, 1943; Makarewicz *et al.*, 2006). The clear supernatant of the protein solution after centrifugation at 13 000 rev min^{-1} at 277 K for 30 min was applied directly onto a 3 ml Ni Sepharose Fast Flow column (GE Healthcare) equilibrated with buffer (20 m*M* Tris–HCl pH 8.0, 100 m*M* NaCl, 1 m*M* $CaCl_2$). The contaminant proteins were washed out with washing buffer (20 m*M* Tris–HCl pH 8.0, 100 m*M* NaCl, 20 m*M* imidazole, 1 m*M* $CaCl_2$). Finally, the target protein was eluted with elution buffer (20 m*M* Tris–HCl pH 8.0, 100 m*M* NaCl, 250 m*M* imidazole, 1 m*M* $CaCl_2$).

The major protein peak was collected, concentrated to 2 ml and applied onto a Superdex G200 (GE Healthcare) size-exclusion chromatography (SEC) column equilibrated with buffer consisting of 20 m*M* Tris–HCl pH 8.0, 100 m*M* NaCl, 1 m*M* $CaCl_2$. The target peak was collected and concentrated to 1 mg ml^{-1} for crystallization.

2.3. Crystallization, data collection and processing

Screening for crystallization conditions took place at 289 K using commercially available kits from Hampton Research (Crystal Screen, Crystal Screen 2, Index, PEG Rx1, PEG Rx2, PEG/Ion and PEG/Ion 2). 1 µl 1 mg ml^{-1} protein solution was mixed with an equal amount of reservoir solution and equilibrated against 80 µl reservoir solution.

Clusters of needle-shaped crystals appeared after 10 d in Crystal Screen condition No. 22 at 289 K. Fine-tuning the pH in the range 7.5–9.5 and the PEG 4000 concentration in the range 25–35% produced crystals that were suitable for diffraction. Streak-seeding was used to improve the quality of the crystals. Seeds obtained by crushing the needle-shaped crystals in stabilizing buffer consisting of 0.2 *M* sodium acetate trihydrate, 0.1 *M* Tris–HCl pH 9.5, 25%(*w*/*v*) polyethylene glycol 4000 were directly applied to a pre-equilibrated 1 µl drop. A suitable single crystal for data collection was finally obtained after 20 d in a condition consisting of 0.2 *M* sodium acetate trihydrate, 0.1 *M* Tris–HCl pH 9.5, 25%(*w*/*v*) polyethylene glycol 4000 at 289 K (Fig. 1).

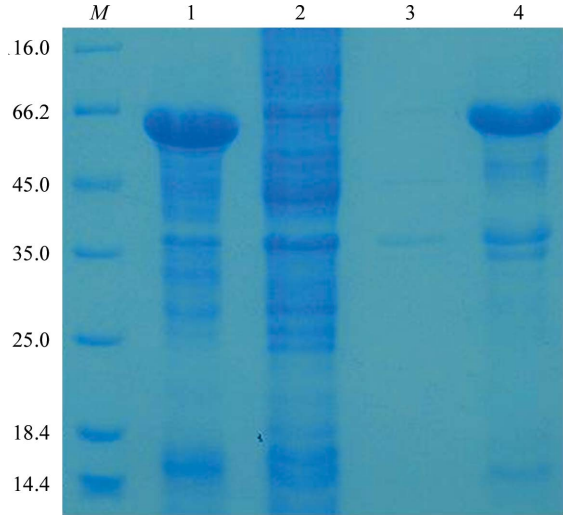

Figure 2
Analysis of soluble renatured protein. Lane 1, pellet after ultrasonication; lane 2, supernatant after ultrasonication; lane 3, pellet after dialysis; lane 4, supernatant after dialysis; lane *M*, protein marker (labelled in kDa).

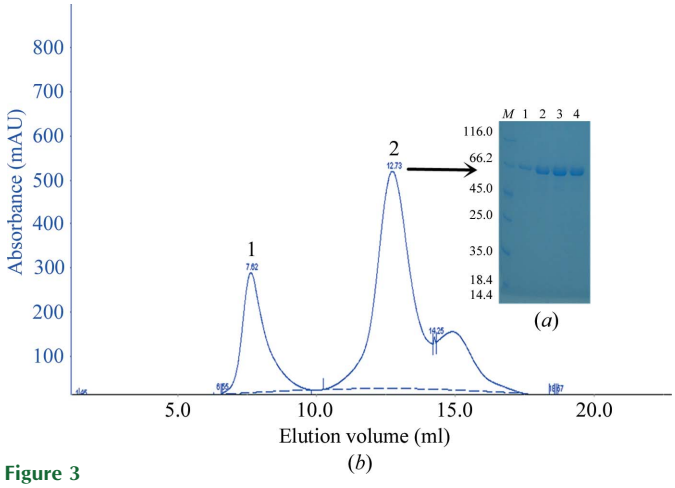

Figure 3
Purification of PhyHT on a gel-filtration column and SDS–PAGE analysis. (*a*) 12% SDS–PAGE stained with Coomassie Brilliant Blue. Lane *M*, protein marker (labelled in kDa); lanes 1–4, PhyHT corresponding to peak 2 on the gel-filtration profile (*b*). (*b*) Purification profile of PhyHT, which eluted as a symmetrical peak from the Superdex G200 SEC column (peak 2).

Table 1
X-ray diffraction data-collection and processing statistics.

Values in parentheses are for the outermost shell.

Space group	$P12_11$
Wavelength (Å)	0.9792
Resolution range (Å)	50.00–2.85 (2.90–2.85)
Unit-cell parameters (Å, °)	a = 46.82, b = 140.19, c = 81.94, α = 90.00, β = 92.00, γ = 90.00
No. of molecules in asymmetric unit	1
No. of observed reflections	151857
No. of unique reflections	22194
$\langle I/\sigma(I)\rangle$	11.72 (2.69)
Completeness (%)	89.9 (79.1)
$R_{\rm merge}$† (%)	17.4 (57.2)

† $R_{\rm merge} = \sum_{hkl}\sum_i |I_i(hkl) - \langle I(hkl)\rangle| / \sum_{hkl}\sum_i I_i(hkl)$, where $\langle I(hkl)\rangle$ is the mean of the i observations $I_i(hkl)$ of reflection hkl.

The havested crystals were quickly mounted on the goniometer in a nitrogen stream at 100 K. Data were collected using a MAR 165 mm CCD detector on beamline 3W1A at the BSRF synchrotron-radiation source, Institute of High Energy Physics, Chinese Academy of Sciences. The data were indexed, integrated and scaled with *HKL*-2000 (Otwinowski & Minor, 1997). The data-collection statistics are listed in Table 1.

3. Results and discussion

The pET-28b-PhyHT co-expression system was constructed and PhyHT was expressed in *E. coli* BL21 (DE3) cells. PhyHT was found to have an apparent molecular weight of 69.3 kDa. The results show that recombinant PhyHT was only detected in the inclusion cell fraction and not in the soluble cell fraction (Fig. 2).

PhyHT was purified to homogeneity, eluting as a symmetrical peak from the Superdex G200 column (Fig. 3*b*) at 12.73 ml elution buffer (peak 2).

The target peak was collected and concentrated to 5 mg ml^{-1} for initial crystallization screening. However, to our great dismay, PhyHT failed to crystallize during initial screening because of precipitation.

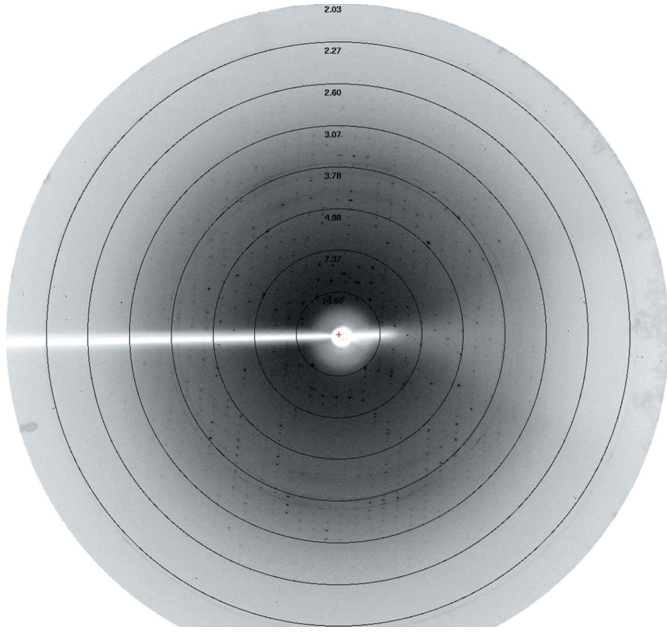

Figure 4
An image of the PhyHT diffraction pattern to a resolution of 2.85 Å.

We decreased the protein concentration to 1 mg ml^{-1} and obtained successful crystallization using Crystal Screen 2 condition No. 43 and PEG/Ion 2 condition No. 41. These results show that the protein can crystallize at low concentrations. We found that streak-seeding could slightly improve the quality of the crystals. Ultimately, fine-tuning the pH and the PEG 4000 concentration of Crystal Screen condition No. 22 produced suitable crystals suitable for diffraction using 0.2 *M* sodium acetate trihydrate, 0.1 *M* Tris–HCl pH 9.5, 25%(*w*/*v*) polyethylene glycol 4000.

The crystal belonged to space group $P12_11$, with unit-cell parameters a = 46.82, b = 140.19, c = 81.94 Å, α = 90.00, β = 92.00, γ = 90.00° (Fig. 4). The asymmetric unit is estimated to contain one molecule of PhyH, with a corresponding Matthews coefficient of 3.88 Å^3 Da^{-1} and a solvent content of 68.31%. Data collection for selenium-derivatized PhyHT and crystal structure determination of PhyHT are in progress.

We thank coworkers at the BSRF for their help in data collection and Dr Zheng Qiang Gao for his help in data processing. This work was supported by the National Natural Science Foundation of China (31070651).

References

Cheng, C. & Lim, B. L. (2006). *Arch. Microbiol.* **185**, 1–13.
Cowieson, A. J., Acamovic, T. & Bedford, M. R. (2004). *Br. Poult. Sci.* **45**, 101–108.
Fu, S., Sun, J. & Qian, L. (2008). *Protein Pept. Lett.* **15**, 39–42.
Gao, W., Lu, F., Li, Q. & Guo, G. (2014). Chinese Patent CN201410006180.4.
Ha, N.-C., Oh, B.-C., Shin, S., Kim, H.-J., Oh, T.-K., Kim, Y.-O., Choi, K. Y. & Oh, B.-H. (2000). *Nature Struct. Biol.* **7**, 147–153.
Holman, W. I. M. (1943). *Biochem. J.* **37**, 256–259.
Kim, O.-H., Kim, Y.-O., Shim, J.-H., Jung, Y.-S., Jung, W.-J., Choi, W.-C., Lee, H., Lee, S.-J., Kim, K.-K., Auh, J.-H., Kim, H., Kim, J.-W., Oh, T.-K. & Oh, B.-C. (2010). *Biochemistry*, **49**, 10216–10217.
Lei, X. G., Porres, J. M., Mullaney, E. J. & Brinch-Pedersen, H. (2007). *Industrial Enzymes: Structure, Function and Applications*, edited by J. Polaina & A. P. MacCabe, pp. 505–529. Dordrecht: Springer.
Li, Z., Huang, H., Yang, P., Yuan, T., Shi, P., Zhao, J., Meng, K. & Yao, B. (2011). *FEBS J.* **278**, 3032–3040.
Makarewicz, O., Dubrac, S., Msadek, T. & Borriss, R. (2006). *J. Bacteriol.* **188**, 6953–6965.
Mullaney, E., Daly, C. & Ullah, A. (2000). *Adv. Appl. Microbiol.* **47**, 157–199.
Otwinowski, Z. & Munor, W. (1997). *Methods Enzymol.* **276**, 307–326.
Pandey, A., Szakacs, G., Soccol, C., Rodriguez-Leon, J. A. & Soccol, V. T. (2001). *Bioresour. Technol.* **77**, 203–214.
Sharma, C. B., Goel, M. & Irshad, M. (1978). *Phytochemistry*, **17**, 201–204.
Shin, S., Ha, N.-C., Oh, B.-C., Oh, T.-K. & Oh, B.-H. (2001). *Structure*, **9**, 851–858.